Original Research

Ultrasound cavitation enhanced chemotherapy: *In vivo* research and clinical application

Zhiyong Shen, Jingjing Shao, Jianquan Zhang and Weixing Qu

Department of Radiology, Affiliated Tumor Hospital of Nantong University, Jiangsu 226361, PR China
Corresponding author: Zhiyong Shen. Email: ntszy259296@126.com

Impact statement

The novelty of this research is that we used ultrasound cavitation to enhance the effects of chemotherapy in the subcutaneous and orthotopic hepatic carcinomas in nude mice. Case reports of the effects of the targeting ultrasound cavitation and chemotherapy on malignant tumors in clinical patients were also examined. We found that low-frequency ultrasound cavitation combined with chemotherapy is effective in the inhibition of tumor growth to some extent.

Abstract

Ultrasound and microbubbles can induce apoptosis of tumor cells. However, the effects of ultrasound and microbubbles (USMB) combined with chemotherapy on *in vivo* tumors have rarely been studied. This research is to evaluate the efficacy of targeted USMB and chemotherapeutic drugs on apoptosis and inhibition of hepatic carcinoma cells in nude mice. We also summarize case reports of its clinical application. It was divided into three parts: First, the subcutaneous hepatic tumors of nude mice were irradiated with ultrasound (20 kHz, 2 W/cm^2, 40% duty cycle) and SonoVue microbubbles injected to the tail vein of the mice followed by chemotherapy comprising cisplatin, mitomycin, and 5-fluorouracil. The apoptosis of hepatoma cells was examined by TUNEL staining, and the expression of the Bax and Bcl-2 proteins in the tumor tissues was detected by immunohistochemistry. The microvasculature of the tumor tissues was observed by transmission electron microscope. Second, orthotopic hepatic tumors in nude mice were irradiated by USMB and chemotherapy. The therapeutic effects were evaluated by magnetic resonance imaging. Third, the malignant tumors in three patients were treated with USMB and chemotherapy. Our results showed that microbubbles focused by low-frequency US ruptured microvessel walls, through which more chemotherapy drugs entered into the carcinoma cells, thus enhancing cell apoptosis, increasing Bax protein expression, and decreasing Bcl-2 expression. The survival period of the nude mice in the USMB and chemotherapy group was the longest, compared with the control, USMB, and chemotherapy (χ^2=29.37, $P < 0.0001$). Magnetic resonance imaging examinations revealed the tumor volumes in nude mice decreased after USMB and chemotherapy ($t = 3.91$, $P = 0.0173$). In clinical cases, after USMB and chemotherapy, the diameters of tumors decreased and the symptoms of the patients were relieved. Targeted low-frequency ultrasound combined with chemotherapy can promote tumor cell apoptosis, inhibit tumor growth, and relieve clinical symptoms of patients.

Keywords: Ultrasound, cavitation, microbubble, chemotherapy, apoptosis

***Experimental Biology and Medicine* 2020; 245: 1200–1212. DOI: 10.1177/1535370220936150**

Introduction

Apoptosis, also known as programmed cell death, refers to the independent and orderly death process of cells controlled by apoptosis-related genes to maintain the stability of the internal environment.[1] The occurrence and development of tumors are due to an imbalance between cell apoptosis and cell proliferation.[2] Induction of apoptosis through different pathways has become a key topic in the antitumor research fields.[3,4]

Studies have shown that ultrasound (US) is one way to induce apoptosis of tumor cells.[5,6] US could induce mitochondrial depolarization, inner mitochondrial membrane permeabilization, and mitochondria-caspase signaling pathway activation[7] along with raised Ca^{2+} concentrations and different expression of caspase-3, Bcl-2, and Bax,[6] thus inducing apoptosis of carcinoma cells. However, the apoptosis index induced by US alone at MHz frequencies (such as 1.75 MHz[7]) is very low (for example 28.33%[7]), and very strong ultrasonic power is necessary (for example

103.7 W/cm^2).[8] However, after adding microbubbles (MBs) and using low-frequency US (20–100 kHz US waves),[9] the energy threshold for tumor cell apoptosis could be significantly decreased. For example, adding SonoVue MBs with 21 kHz US, and 30 s sonication time, the required US energy is only 46 mW/cm^2 to induce apoptosis in human prostate cancer cells.[10] The main mechanism of low-frequency US is thought to be the cavitation effect.[11] Cavitation refers to the phenomenon of expansion, contraction, and collapse of MBs under the action of ultrasonic fields.[12] Low-frequency US combined with MBs (USMB) could induce the cavitation effect to produce sonoporation, thus enhancing gene transfection to induce cell apoptosis.[13] In the process of cell apoptosis, mitochondrial depolarization, mitochondrial permeability via transition pore opening, and cytochrome c release occur.[14] USMB can also enhance cell apoptosis in subcutaneous tumors in nude mice.[15,16]

Cisplatin (DDP),[17] mitomycin (MMC),[18] and 5-fluorouracil (5-FU)[19] are commonly used chemotherapeutic drugs in clinical applications, and each one can accelerate cancer cell apoptosis and restrain tumor growth. However, USMB combined with multiple chemotherapeutic agents to treat tumors has not been extensively studied.[20]

This study is divided into three parts: In the first part, subcutaneous xenografts in nude mice were subjected to 20 kHz US combined with SonoVue MBs for two weeks, followed by injection of the chemotherapeutic agents (DDP+MMC + 5-FU, PMF scheme) into the tail vein for another two weeks to explore the effects of USMB+PMF on apoptosis in hepatic carcinoma cells (Figure 1). In the second part, the effects of USMB+PMF on orthotopic liver carcinoma in nude mice were studied. There are few cavitation nuclei in the vasculature of the normal human body.[21] Intravenously injected MBs can increase the number of cavitation nuclei in the body to enhance the cavitation effect on tumor therapeutic targets.[22] Finally, in the third part, case reports on the effects of USMB and chemotherapy on malignant tumors in clinical patients are examined. The aim of this study is to explore the enhancing effects of chemotherapy by targeted cavitation induced with USMB.

Materials and methods

Animal protocol

All of the nude mice were aged five to six weeks, weighed 20–22 g, and were purchased from Shanghai Slack Experimental Animal Co., Ltd (production license (Shanghai 2017–0005)). They were kept in specified pathogen-free (SPF) animal rooms at the Nantong University Animal Experiment Center (use license (Su 2017–0046)), and they were provided *ad libitum* sterilized water and feed. Animal feeding and treatment were approved by the animal ethics committee of the Animal Center of Nantong University.

Subcutaneous tumor model establishment. After intraperitoneal application of 70 mg/kg sodium pentobarbital, each mouse was subcutaneously injected with 1×10^7 HepG2 carcinoma cells. The mice were fed again under SPF conditions. Fifteen days later, the research started when the tumors had attained a size in diameter of 6–7 mm.

Ultrasound instruments and MBs. The ultrasonic therapeutic apparatus (Jiangsu Han Mei biotechnology, Taizhou, China) has a transmitting frequency of 20-kHz, a sound intensity of 2 W/cm^2, and a duty cycle of 40% (on 2 s, off 3 s). The MBs used were an ultrasound contrast agent (SonoVue: Bracco SpA, Milan, Italy) and the bubble suspension consisted of 59 mg sulfur hexafluoride and 5 mL saline. The MBs dose of tail vein injection each time for each mouse is 0.2 mL. The ultrasonic intensity (2 W/cm^2) has been set and fixed by the manufacturer. We choose a frequency of 20 kHz, because the lower the ultrasonic frequency, the stronger the cavitation effect;[23] 20 kHz ultrasound is actually in the lowest frequency range of ultrasound. Theoretically, its ultrasonic wave can produce the strongest cavitation effect. We used pulse waves with the duty cycle of 40% for the following reasons. First, it was reported that continuous wave ultrasound theoretically emphasizes thermal bio-effects, whereas the pulsed ultrasound emphasizes cavitation.[21] Second, the time set of on 2 s and off 3 s is easy to operate and control manually. We injected MBs into the tail vein of mice, which not only increased the cavitation nucleus, but also reduced the cavitation threshold.[24]

The probe was placed on the subcutaneous tumors of the mice, with an ultrasound transmission gel to ensure US propagation (Figure 2(a)). The sonication time was 1 min once every other day for two weeks.

Chemotherapy drugs

The chemotherapeutic drugs used were DDP (1 mg/kg), MMC (0.5 mg/kg), and 5-FU (5 mg/kg). Before injection of the chemotherapeutic drugs, the tail veins of the nude mice were injected with an indwelling needle (BD Intima II rema closed venous indwelling needle, Yangzhou Jian Xin medical instrument Co., Ltd, Yangzhou, China). The indwelling needle was 24 G × 0.75 with a needle tip of 0.7 mm × 19 mm (Figure 2(b)). When venous blood reflux was observed, the needle core was slowly pulled out and the outer soft tube was left in the tail vein of nude mice fixed with mackintosh (Figure 2(c)). The drug concentrations were adjusted according to the dose used; 0.2 mL DDP (concentration 0.1 mg/mL), 0.2 mL MMC (concentration 0.05 mg/mL), and 0.2 mL 5-FU (concentration 0.5 mg/mL) were injected into the soft tube in the tail vein. The chemotherapeutic mixture, DDP+MMC+5-FU (PMF), was injected into the tail veins once every other day for two weeks.

Groups

Forty-eight subcutaneous tumor model mice were randomly divided into 4 groups, with 12 mice in each group. The groups comprised group A, control (sham treatment); group B, the USMB group, with 0.2 mL SonoVue MBs injected into the tail vein of nude mice (the tumor was simultaneously irradiated by 20-kHz US for 1 min, once every other day for two weeks); group C, the chemotherapy

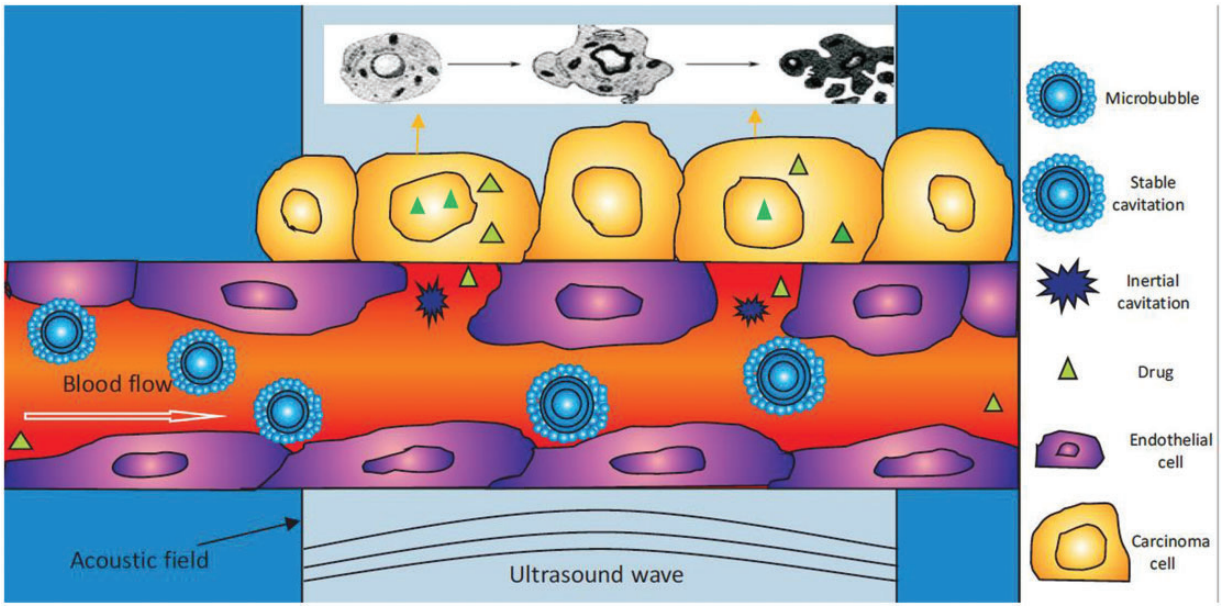

Figure 1. Scheme of the therapeutic mechanism of USMB+PMF. (A color version of this figure is available in the online journal.)

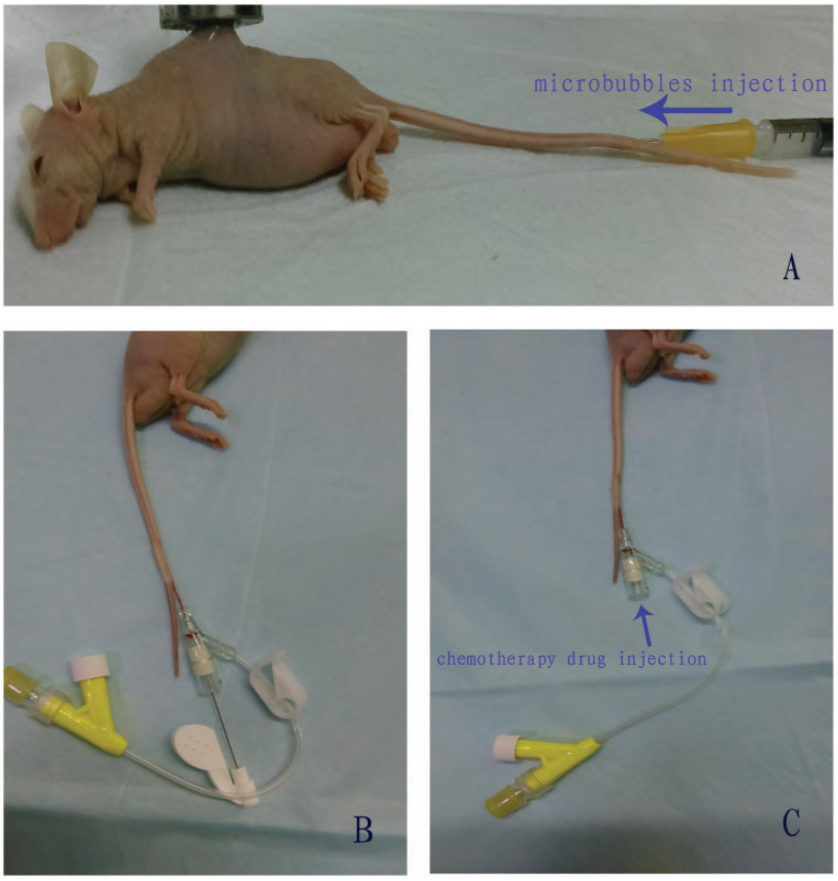

Figure 2. (a) Subcutaneous tumor of nude mice treated by 20-kHz ultrasound and microbubbles. (b) Insertion of an indwelling needle into the tail vein of a nude mouse. (c) After blood reflux, the needle core is removed leaving the soft tube (hose) from outside the needle core in the tail vein. (A color version of this figure is available in the online journal.)

group, in which the three drugs, 0.2 mL DDP+ 0.2 mL MMC+ 0.2 mL 5-FU (PMF), were sequentially injected, once every other day for two weeks, slowly into the soft venous indwelling catheter in the tail vein of nude mice at the speed of 0.04 mL/s, and after which, the indwelling catheter was removed and the hemostasis was stopped by vein compression; and group D, the USMB+PMF group (two weeks of USMB followed with 2 weeks of PMF).

The reason why we use treatment sequence USMB + PMF is as following. In order to break the tumor vessel wall, ultrasound combined with bubble irradiation must be performed for a certain time such as a duration of a few weeks. If the tumor is irradiated by ultrasound at the same time when the chemotherapy drugs are injected intravenously, sonication may not be able to break the tumor blood vessels, because there is not enough irradiation time. In addition, if chemotherapy was carried out for two weeks first, followed by ultrasound bubble irradiation for two weeks, the chemotherapy drugs in mice would have already been metabolized, and USMB would have no effect at all. So, we think that USMB+PMF is the optimum sequence.

Our previous study found that two-week irradiation by ultrasound combined with bubbles is enough to damage tumor blood vessels.[25] On the other hand, according to our experience in animal experiments, because the tail vein of nude mice is vulnerable to rupture and not easy to recover, the two tail veins of each nude mouse can only endure injection for up to 12 times (4 weeks), so we choose the longest treatment time with 2 weeks USMB + 2 weeks PFM.

After completion of therapeutic experiment, 24 mice, 6 mice randomly taken from each group, were euthanized, and the subcutaneous tumors were gathered, cut into three sections for cell apoptosis detection, immunohistochemistry, and transmission electron microscopy (TEM). The remaining 24 mice, 6 mice in each group, were saved and fed continuously, and the overall survival time was calculated.

Cell apoptotic protein detection

The apoptotic cells were tested by terminal deoxynucleotidyl transferase-mediated dUTP-biotin nick end labeling (TUNEL). The TUNEL kit (POD) was purchased from Roche Molecular Biochemicals. The assay was performed as per the technical manual and Liu *et al*.[26] The apoptotic index (AI: percentage of TUNEL-positive cells) was calculated as the number of TUNEL-positive cells/the total number of cancer cells $\times 100\%$.

Immunohistochemistry staining

Rabbit monoclonal antibodies against human Bcl-2 (1:100 dilution) and Bax (1:50 dilution) were purchased from Zhongshan Goldenbridge, Beijing, China. The expression of the Bax and Bcl-2 proteins was localized in the cytoplasm of tumors and positive expression was manifested as pale yellow, brown-yellow or brown. The cells were scored according to the percentage of positive signal in the cytoplasm and divided into the following classes: score 0, $<5\%$; score 1, 5–25%, score 2, 26–50%; score 3, 51%–75%; score 4, $>75\%$.[27] The degree of cytoplasmic staining was scored according to the following classes: score 0, no staining; score 1, pale yellow; score 2, brown yellow; score 3, brown.[27] The total score was the score of the staining percentage multiplied by the score of the staining degree.

Transmission electron microscopy

Each tumor sample, $\sim$1 mm^3, for TEM was fixed in 2% glutaraldehyde. After treatment with 1% osmium tetroxide in PBS, specimens were dehydrated with ethanol. The samples were then embedded in propylene oxide and stained with lead citrate E. Finally, the specimens were examined using TEM (Philips CM-120; Philips, Eindhoven, The Netherlands).

Survival time follow-up

The survival time was calculated based on the date of tumor incubation and the date of death. At the end of the experiment, the survival times of the 24-treated nude mice in each group of six euthanized mice was calculated using a right censoring survival model. The survival times of the remaining 24 nude mice in each group of six mice was followed up.

Establishment of orthotopic hepatic carcinoma models in nude mice

One nude mouse was subcutaneously injected with 0.2 mL (1×10^7 cells) of a cell suspension from the HepG2 cell line. Two weeks later, orthotopic hepatic carcinoma models were performed. The subcutaneous tumor was removed from the nude mouse under aseptic conditions. The tumor tissue was cut into approximately 1 mm^3 pieces. All five nude mice were anesthetized with 70 mg/kg pentobarbital; 0.2% iodophor was used to disinfect the upper abdomen of the nude mouse. A right oblique incision of the costal margin of approximately 2 cm was made to open the abdominal cavity and expose the liver. A needle on a 10 mL syringe was inserted into the liver capsule at an angle of approximately 15° to the right lobe of the liver. The depth of the pierced tunnel was approximately 0.6 cm, and an aseptic cotton swab was pressed on the wound for 8 s to stop the bleeding. One piece of carcinoma tissue was placed into the right lobe of the liver in the recipient mice. Approximately 0.05 mL alpha cyanoacrylate rapid medical adhesive (OB medical adhesive glue, Guangzhou Baiyun medical adhesive Co., Ltd, Guangdong, China) was immediately instilled into the tunnel outlet to ensure that there was no overflow of the tissue piece and no bleeding. Finally, the abdominal cavity was closed layer-by-layer. The average operation time of each nude mouse was 6–8 min. The nude mice were awakened gradually after anesthesia for 30–40 min and then returned to the cages under SPF conditions. In total, five orthotopic nude mice models of liver cancer were established. Six weeks later, magnetic resonance imaging (MRI) was performed to judge the effect of model establishment.

MRI

The MRI scans of the orthotopic hepatic tumors in the mice were acquired in the Department of Imaging of the Nantong Tumor Hospital using a 3.0 Tesla MRI scanner (3.0 T coil, Siemens Espree, Germany) with a small animal coil. The examination was performed four weeks after tissue implantation. The animals were given 70 mg/kg

pentobarbital intraperitoneally. After administration of anesthesia, the nude mice were put into animal coils (Figure 3) for MRI examination. Cross-sectional T2-weighted images were acquired with the following parameters: T2 propeller sequence; slice thickness, 0.6 mm; slice spacing, 1 mm; TR, 3140 ms; TE, 81 ms; FOV, 64 mm × 64 mm; base resolution, 256. After MRI examination, orthotopic hepatic tumorigenesis of nude mice was successful. Then, the treatment for orthotopic liver cancer of mice was started. The therapeutic regime was the same as the treatment in group D of subcutaneous mice model research. That was the schedule of two weeks of USMB followed with two weeks of PMF. No mice served as control. After four weeks treatment (USMB+PMF), each orthotopic hepatocellular carcinoma in nude mice was examined by MRI again to judge the therapeutic effects.

Because the shape of the orthotopic tumors is close to sphere, we use the formula $(4/3\pi(d/2)^3)$ to calculate the tumor volume, in which d is the diameter of the tumor.

Clinical population

Three patients suffering from malignant carcinomas were treated with USMB combined with chemotherapy. The therapy of the patients was approved by the ethics committee of affiliated Tumor Hospital of Nantong University. Written consent was obtained from the patients. The carcinoma histories, diagnoses and imaging are shown in Table 1. Before treatment, the bleeding time and coagulation time in the serum were tested as they must be in the normal range for US treatment.

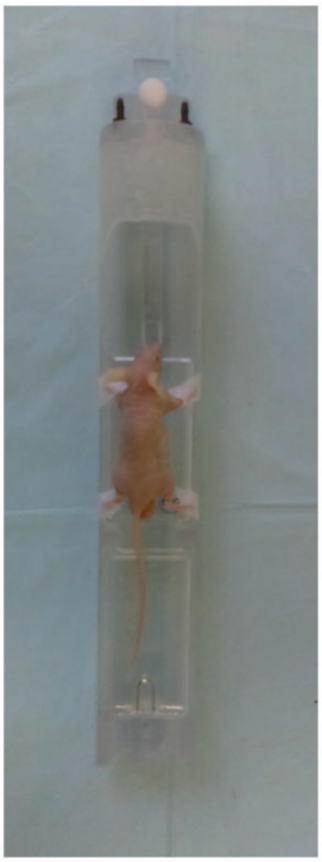

Figure 3. Nude mouse coil. (A color version of this figure is available in the online journal.)

US sonication process

The patients were in the supine or left lateral position. An iU22 ultrasound system (Philips, Bothell, Washington, USA) was used to locate the tumors and determine the direction of ultrasonic irradiation (emitting angle) before their treatment. The probe frequency for scanning the abdominal organs was 3 MHz, and the probe frequency for superficial organs was 12 MHz. According to the body surface location guided by the diagnostic ultrasound, one to three therapeutic points on the body surface facing the targets were selected according to the tumor number, size, and location (the distance between the two points was at least 3 cm). Hepatic tumors or abdominal wall tumors were subsequently sonicated using a transducer the same as in the animal experiments. The US parameters were set to 20 kHz, 2 W/cm^2, and 40% duty cycle (2 on, 3 off). Carbon dioxide (CO_2) MBs were used as they were less expensive than SonoVue bubbles.

CO_2 bubbles can be used as cavitation nuclei,[28–30] as they implode and damage blood vessels under the irradiation of an external sound field.[30]

The formula for the CO_2 MBs is as follows; 100 mL of 0.9% sodium chloride was used to establish an intravenous infusion channel in the treatment process at 60 drops per minute. The CO_2 MBs were composed of 20% vitamin C 4 mL + 5% sodium bicarbonate 10 mL + hydroxyethyl starch 10 mL and were injected into the intravenous infusion channel within 30–60 s. Ultrasound radiation therapy was performed after injection of the CO_2 MB agent (Figure 4). The targeted zones of the tumors were subjected to ultrasonic radiation for 10 min. Ten minutes later, a second injection of CO_2 MBs was given followed with a repeat of the sonication. Each patient underwent treatment three times a day for approximately 30 min. After treatment, the patients received an IV drip with 250 mL 0.9% sodium chloride + 2.0 g etamsylate + 0.2 g aminomethylbenzoic acid. One course of the treatment was five days with two days of rest.

Chemotherapy regimen

In case 1, the patient was treated with intravenous oxaliplatin 130 mg/m^2 on day 1 plus oral capecitabine 1000 mg/m^2 twice daily on days 1–14. In case 2, chemotherapy was composed of intravenous oxaliplatin 130 mg/m^2 and calcium folate 200 mg/m^2 and followed by 500 mg/m^2 5-FU as a 24-h continuous infusion i.v. In case 3, chemotherapy consisted of 50 mg/m^2 Epirubicin infusion i.v. on day 1 and 30 mg/m^2 cisplatin i.v. as a 2-h infusion on days 1–3 and followed by 500 mg/m^2 5-FU as a 24-h continuous infusion i.v. on days 1–5. Due to the different medical histories, different tumor stages, and different economic abilities for different patients, different chemotherapy schemes are adopted, which are all commonly used chemotherapy schemes for gastrointestinal cancers.

Table 1. Clinical cases including history, diagnosis, therapy, and imaging findings (clinical case reports of low-frequency US and MBs combined with chemotherapy for patients suffering malignant tumors).

Case	History	Before treatment	USMB	Chemotherapy	After treatment	Patient's symptoms
1	Male, 70ys old, Abdominal discomfort for 3 months, after gastric cancer surgery	CT: multiple liver metastasis	20 kHz US+ bubbles for 10 days	Oxaliplatin + capecitabine	CT: decreased size of hepatic metastasis and upper abdominal lymph node	Relieved abdominal distention and pain
2	Male, 68ys old, 3 months of abdominal pain in the upper abdomen	Gastroscopy: duodenal neoplasm. Pathology: adenocarcinoma CT: hepatic metastasis	20 kHz US+ bubbles for 10 days	Calcium folate +5-FU + oxaliplatin	CT: decrease in the number of liver metastases	Abdominal pain obviously alleviated
3	Male, 59ys old, 6 months after resection of gastric cancer, abdominal pain for 2 months	PET-CT: abdominal wall metastasis 2.4 cm	20 kHz US + bubbles for 10 days	EPI +DDP +5-FU	PET-CT: mass size decreased to 1.8 cm	Abdominal wall pain relief

CT: computed tomography; USMB: ultrasound combined with CO_2 microbubbles; EPI: epirubicin; DDP: cisplatin; 5-FU: 5-fluorouracil; PET-CT: positron-emission tomography computed tomography.

Computed tomography

Two patients were examined by CT before and after therapy. CT was performed using a 64-section multidetector CT scanner (Somatom Sensation 64; Siemens Medical Systems, Erlangen, Germany).[31]

Positron emission tomography imaging method

One patient was examined by ^{18}F-fluorodeoxyglucose positron-emission tomography/low-dose computed tomography (^{18}F-FDG PET/CT) (Philips, Amsterdam, The Netherlands). The CT scanning parameters were as follows: voltage, 140 kV; current, 90 mA; 0.8 s per period/cycle; layer thickness 5 mm; bed speed 22.5 mm/s; matrix 512×512; image fusion to 128×128. Parameters of the PET for the 2D scan: matrix 128×128; a total of 2–6 window collection; each collection for 3–5 min.

Statistical analysis

The results were expressed as the mean $\pm$ SD. The data were analyzed by Student's *t*-test. The survival curves were calculated using the Kaplan–Meier method and were analyzed using the log-rank test. Values of $P < 0.05$ were considered significant.

Results

TUNEL results

Apoptotic cells showed a nuclear-positive phenotype, that is, the nuclei were brown. Under light microscopy, different proportions of apoptotic cells were found in each group. Typical apoptotic cells had nuclear condensation, dense nuclei, deep staining, and brown nuclei. The nuclei of non-apoptotic cells were blue (Figure 5). The average apoptosis rates of the tumor cells in the control, USMB, PMF and USMB+PMF groups were 8 ± 5, 43 ± 11, 47 ± 11 and 79 ± 11%, respectively. There were statistically significant differences between the USMB+PMF group and the control, USMB, and PMF groups with $t = 13.41$, $P < 0.0001$; $t = 5.81$, $P = 0.0021$; and $t = 3.63$, $P = 0.0151$, respectively (Figure 6).

Immunohistochemistry staining results

The average Bax scores of the tumor cells in the control, USMB, PMF, and USMB+PMF groups were 3.33 ± 1.515, 6 ± 1.798, 6.667 ± 1.632, and 9.833 ± 2.563, respectively (Figure 7). There was a significant difference between the USMB+PMF group and the control, USMB, and PMF groups with $t = 5.8138$, $P = 0.0021$; $t = 4.6$, $P = 0.0058$; and $t = 3.48$, $P = 0.0176$, respectively (Figure 8). The average Bcl-2 scores of the tumor cells in the control, USMB, PMF, and USMB+PMF groups were 6.1667 ± 2.0412, 4.5 ± 2.168, 4 ± 1.673, and 2.333 ± 1.0327, respectively (Figure 9). There was a significant difference between the USMB+PMF group and the control, USMB, PMF groups with $t = 4.838$, $P = 0.0047$; $t = 3.3127$, $P = 0.0212$; and $t = 2.988$, $P = 0.0305$, respectively (Figure 10).

Figure 4. The tumor was treated with 20-kHz ultrasound, after injection of CO_2 microbubbles into the ulnar vein. (A color version of this figure is available in the online journal.)

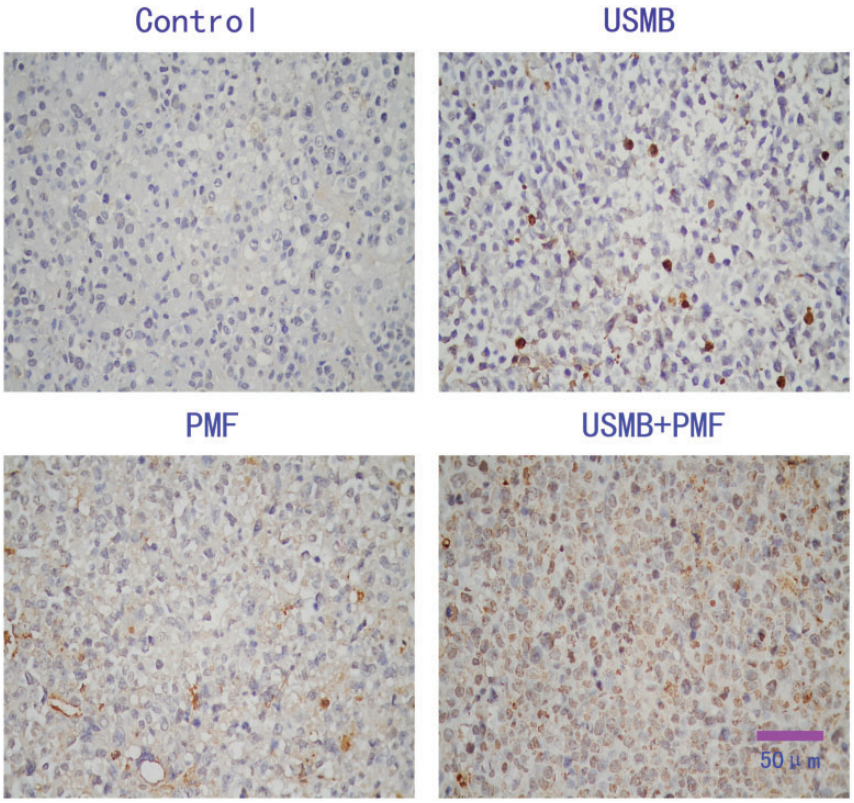

Figure 5. TUNEL staining in four groups (control, USMB, PMF, and USMB+PMF) of tumor cells (×200). (A color version of this figure is available in the online journal.)

TEM results

TEM of the USMB and USMB+PMF samples revealed vascular endothelial cell wall rupture, widened endothelial cell gaps, and interstitial erythrocyte leakage, while intact vascular endothelial cells and normal erythrocytes in the tumor vessels were observed in the control and PMF groups (Figure 11).

Survival time follow-up results

The average survival time of the nude mice in the control, USMB, PMF, and USMB+PMF groups were 48 ± 8, 56 ± 16, 57 ± 18, and 68 ± 31 days, respectively. The survival times of ultrasound followed with chemotherapy group was longer (the longest time was 124 days). Mice treated with USMB+PMF had a significantly longer overall survival time than those in the control, UBMB, and PMF groups (χ^2=29.37, $P < 0.0001$) (Figure 12).

The results of orthotopic hepatic carcinoma treated with USMB and chemotherapy

The tumor volumes of the orthotopic hepatic carcinomas in the nude mice were calculated by MRI. The treated orthotopic hepatic carcinomas in the nude mice were compared to the untreated condition. The tumor volume of the orthotopic hepatic carcinomas in nude mice before USMB+PMF was 275.17, 573.81, 205.36, 161.75, and 765.52 mm^3 respectively. The tumor volume of the orthotopic hepatic carcinomas in nude mice after USMB+PMF was 110.85, 386.81, 58.63, 124.18, and 458.91 mm^3, respectively. In the comparison between pre-treatment and post-treatment, there was a

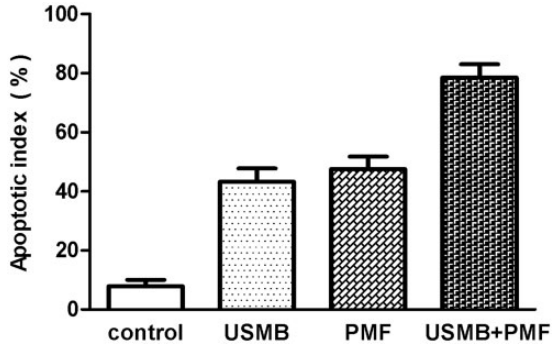

Figure 6. Apoptosis index in the control, USMB, PMF, and USMB+PMF.

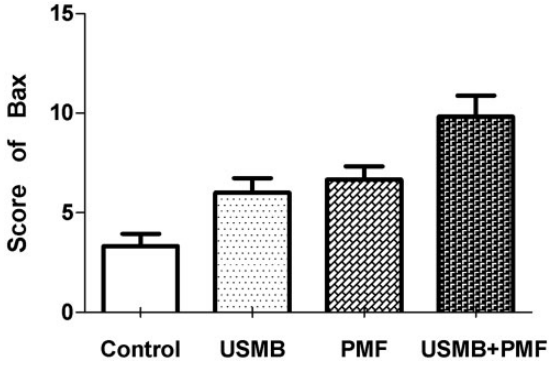

Figure 8. Bax protein scores in the four groups.

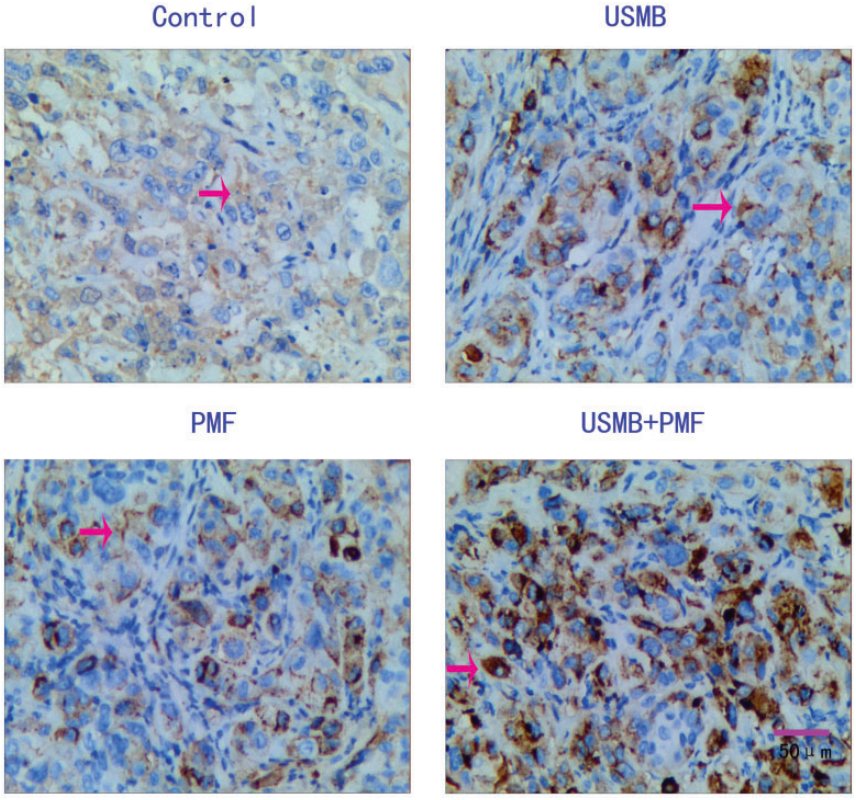

Figure 7. Bax expression in tumor cells from the 4 groups (×200) (arrow: positive staining). (A color version of this figure is available in the online journal.)

statistically significant decrease in tumor size ($t = 3.91$, $P = 0.0173$) (Figure 13).

The results of clinical application of USMB and chemotherapy

No side effects, such as fever and bleeding were observed during or after the 20-kHz US and MBs treatment. In cases 1 and 2, after USMB + chemotherapy, the hepatic metastasis size decreased on CT (Figure 14). The symptoms of abdominal distention and abdominal pain in the two patients were relieved. In case 3, before therapy, the ^{18}F-FDG PET/CT exam showed high glucose metabolism in the abdominal wall tumor, which was diagnosed as a malignant metastasis. After USMB + chemotherapy, the abdominal wall tumor metastasis size decreased on PET/CT (Figure 15). Table 1 shows that the low-frequency US combined with chemotherapy reduced the liver tumors in cases 1 and 2 and reduced the metabolic activity and the diameter of the abdominal wall tumor in case 3. These results showed that low-frequency US combined with chemotherapy can inhibit tumor growth in clinical patients.

Discussion

MBs irradiated by 20-kHz US resulted in rupture of tumor vessels

TEM revealed that the tumor microvessel walls ruptured in the USMB+PMF and USMB groups and that red blood cells leaked into the tumor interstitial tissue. The intravascular SonoVue MBs in the tumor vessels were irradiated by 20-kHz US, and as a result the MBs expand, contract, implode intensely, and then burst. The resulting cavitation effect releases a large amount of energy[32] that eventually leads to microvasculature damage and rupture. In the control and PMF groups, no bubble was given to animal tail veins and no ultrasound irradiation was applied; therefore, no cavitation was produced. As a consequence, the tumor microvascular walls clearly had no defects.

USMB followed by chemotherapy increased tumor cell apoptosis and inhibited tumor growth of nude mice

The target of the chemotherapy drug cisplatin is the DNA structure in tumor cells, and resulting changes can interfere with DNA repair[33] in carcinoma cells. Mitomycin can enhance the expression of caspase-3 protein to induce

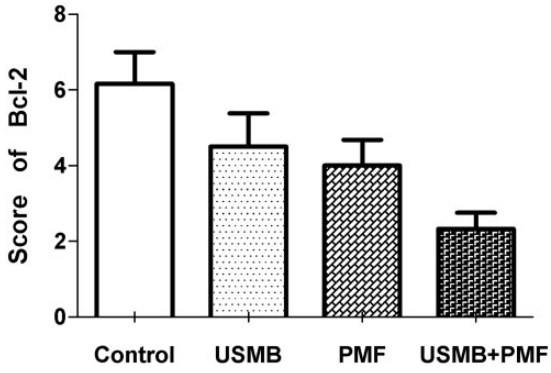

Figure 10. Bcl-2 protein scores of tumor cells from the four groups.

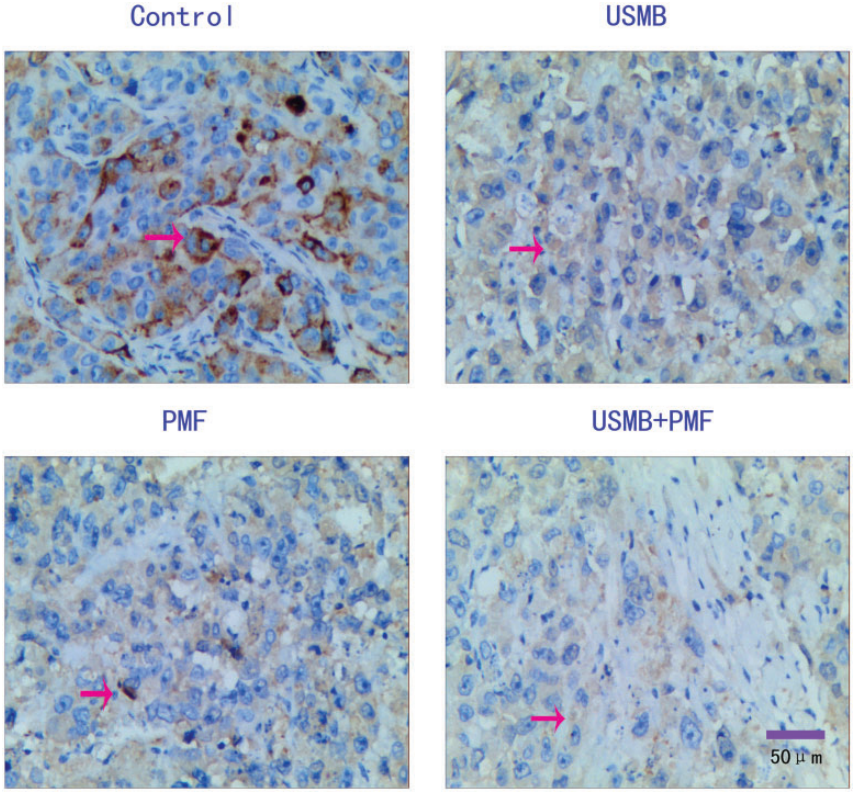

Figure 9. Bcl-2 expression in four groups (×200) (arrow: positive staining). (A color version of this figure is available in the online journal.)

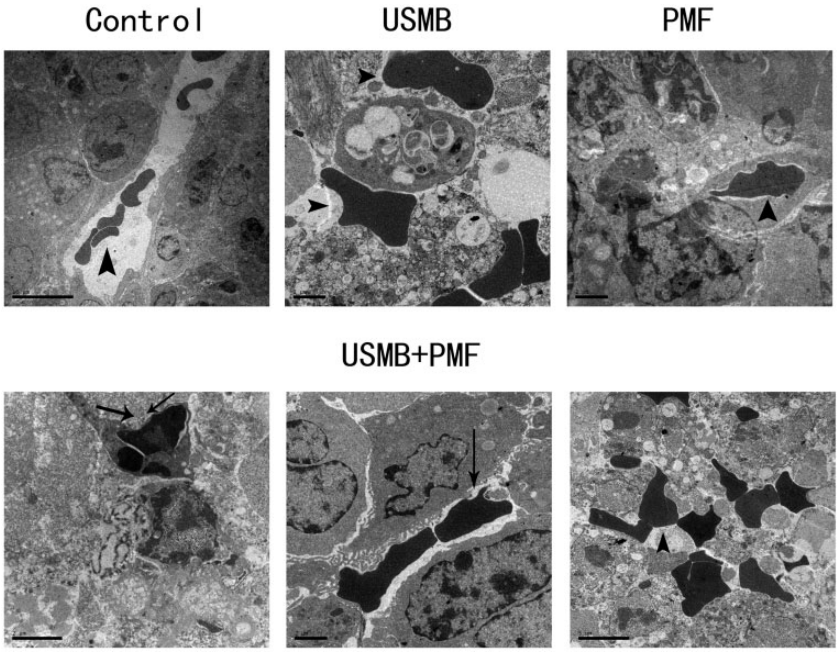

Figure 11. TEM results of tumor vessels in the four groups (arrow head: red blood cell; arrow: rupture of vascular wall).

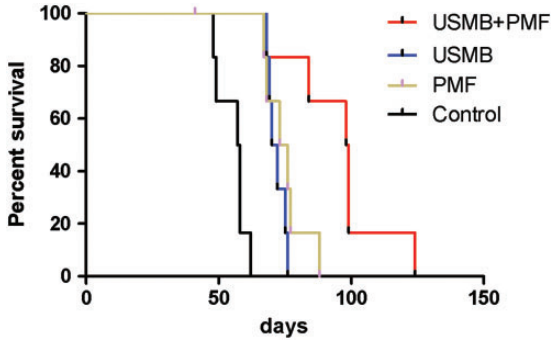

Figure 12. The survival time curve of the nude mice in the four groups. (A color version of this figure is available in the online journal.)

apoptosis of the hepatoma cells.[34] 5-FU interferes with cellular RNA and inhibits thymidine deoxyribonucleotide synthetase, thus hindering DNA synthesis.[35] Combined chemotherapy can enhance cellular oxidative stress, DNA damage, mitochondrial apoptosis, and death receptor signaling.[36] After irradiation with US MB, the tumor vascular walls were injured and ruptured by the shock waves and jet streams induced by inertial cavitation in the nude mice.[37,38] Chemotherapy drugs were given to the animal tail veins. DDP, MMC, and 5-FU entered into the tumor cell tissue through the broken areas of the microvessels produced by the cavitation effect, killing the carcinoma cells and promoting cell apoptosis (Figure 1). Therefore, the apoptosis in the USMB + PMF group was higher than that in the other three groups. In the PMF alone group, the blood vessel walls were intact and lower amounts of chemotherapeutic drugs could enter the tumor tissue; therefore, the apoptosis rate in the PMF group was lower than that in the USMB + PMF group. In the USMB group, no chemotherapy drugs were injected, so the apoptosis rate was also lower than that in the USMB+PMF group.

Bcl-2 plays an important part in apoptosis.[39] The Bcl-2 protein has an anti-apoptotic role, while Bax promotes tumor cell apoptosis.[40] Our research disclosed that Bax protein in the USMB+PMF group was higher than that of the other three groups, while Bcl-2 was lower than that of the other three groups. Therefore, the apoptosis of the tumor cells in the USMB+PMF was more, indicating that the proliferation of the cancer cells was more restrained and the tumor growth was therefore inhibited. As a consequence, the nude mice had a longer survival period.

Comparison with other related studies

Ren *et al.*[41] performed ultrasound (0.8 MHz, 2.79 W/cm^2) irradiated MBs loaded with docetaxel injected into the tail veins of nude mice. After treatment, the subcutaneous H22 HCC growth was significantly inhibited, proliferating cell nuclear antigen expression in carcinoma tissue decreased and local release of docetaxel increased.[41] Liu *et al.*[42] used ultrasound (30 kHz) and paclitaxel to sonicate subcutaneous EMT6 breast carcinoma models in nude mice. US and chemotherapy increased the local concentrations of paclitaxel in the tumors and restrained tumor volume in transplanted subcutaneous EMT6 carcinomas.[42] Hu *et al.*[20] found that US (1.1 MHz, 1.0 W/cm^2, 10% duty cycle) combined with 5-FU could lead to the growth inhibition of hepatic carcinoma in nude mice.[20] Compared with Ren *et al.*,[41] Liu *et al.*,[42] and Hu *et al.*,[20] the frequency of ultrasound we used is lower (20 kHz). Theoretically, sound waves with lower frequencies have longer periods leading to longer MB oscillation time in the expansion phase and a larger expansion in the diameter of the MBs.[43] The greater the damage effect in the compression phase,[43] the more obvious the cavitation effect we had. In addition, while they used a single drug, either paclitaxel or docetaxel, we used three chemotherapeutic drugs, DDP, MMC, and 5-FU,

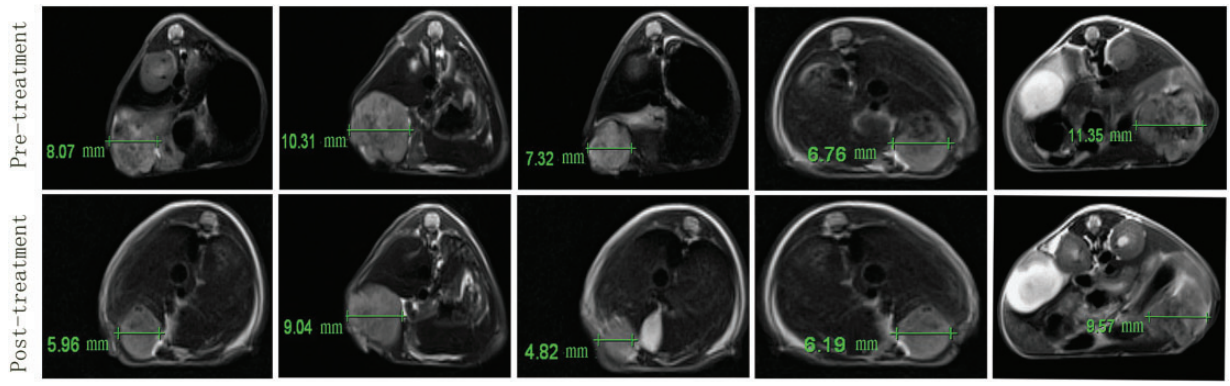

Figure 13. MRI measurement of tumor diameter before and after treatment with USMB+PMF in orthotopic hepatocellular carcinoma in nude mice. (A color version of this figure is available in the online journal.)

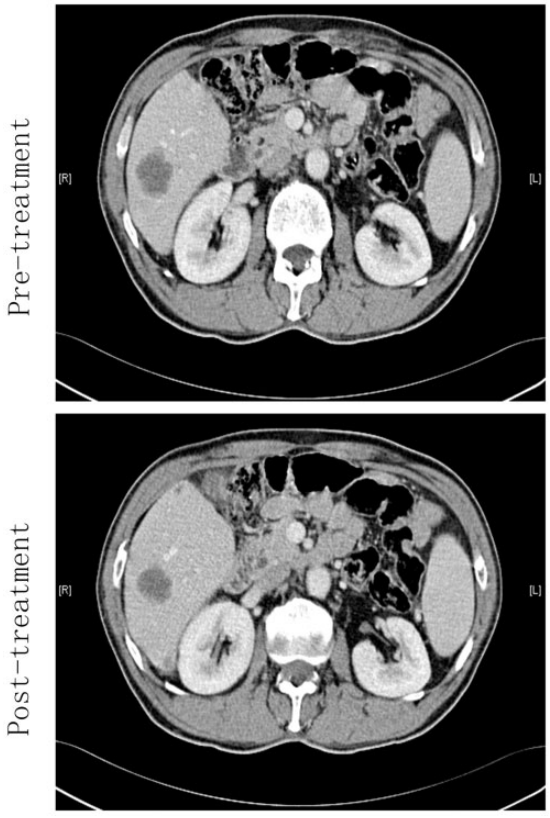

Figure 14. Clinical case number 1. CT scan before and after 20-kHz ultrasound with chemotherapy for the tumors.

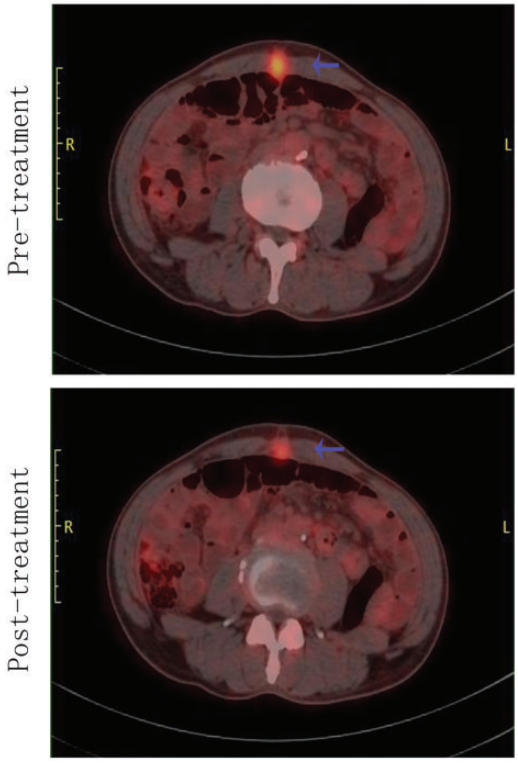

Figure 15. Clinical case number 3. PET-CT results before and after 20-kHz ultrasound with chemotherapy for the abdominal wall tumor (arrow: tumor). (A color version of this figure is available in the online journal.)

which is more consistent with the clinical practice of multi-drug combination usage.[44]

USMB and chemotherapy inhibited orthotopic hepatic carcinoma in nude mice

The method of subcutaneous model establishment is simple and we can directly observe the growth of tumors. The orthotopic transplantation hepatocellular carcinoma mouse models could reveal the growth state and invasion behavior of hepatic carcinoma,[45] which is very similar to the biological behavior of human hepatocellular carcinoma.[46]

As the subcutaneous tumors were examined at the cellular level; more apoptosis was found, which proves that USMB + PMF is effective. Therefore, in orthotopic tumor models, we pay attention to the therapeutic effects at macroscopic and general levels; that is, we use MRI to observe the volume changes, rather than the repetitions of TUNEL test and immunohistochemistry.

In this study, MRI showed that the tumor volume decreased after USMB+PMF treatment (Figure 13), indicating that a combination of low-frequency US and chemotherapy could also inhibit the tumor growth of orthotopic hepatic carcinoma in nude mice.

Clinical application of USMB and chemotherapy

Clinical application of low-frequency US is rare. Ai[29] *et al.* retrospectively analyzed 25 patients with malignant hepatic tumors treated by radiofrequency ablation (RA) combined with US and MBs. They found that the therapy of hepatic carcinoma by RA+USMB is effective and safe, and can cause tumor recession and protect liver function.[29] Quality of life scores of most patients (92%) were good or improved.[29] The mechanism of RA+USMB is that RA damaged cancer tissue and tumor vessels, while USMB destroyed tumor microcirculation.[29] In our previous research,[47] a hepatic tumor in an old man was treated with USMB. After therapy, the intensity and enhanced areas of the tumor on the CT examination and contrast-enhanced US decreased.[47] In this study, we further studied the effects of USMB combined with chemotherapy; 20-kHz ultrasound is characterized by low frequency, long wave, low attenuation in the tissue, strong penetration, and can reach the deep tumor of human body. Each time before the tumor treatment, its location is carried out by diagnostic ultrasound to be accurately focused. In our research, three patients suffering advanced-stage malignant tumors were treated with USMB and chemotherapy. It was found that this treatment could reduce the tumor size in the irradiated area, relieve the symptoms of the patients, and improve their quality of life. Case 3 suggests that low-frequency US is not only useful for irradiating deep-seated tumors such as liver carcinoma but is also useful for superficial-seated ones such as abdominal wall tumors, which expanded the tumor location range.

The shortcoming of this study is that it includes only a few clinical cases, although the results do show that the cancer treatment has a definite effect. In the future, a larger clinical data set is needed to further confirm the efficacy of USMB + chemotherapy.

Conclusion

In conclusion, the cavitation effect produced by US and MBs destroys tumor blood vessels, allowing the chemotherapeutic drugs to enter the tumor tissue through the ruptured vessels. This technology promotes apoptosis of the tumor cells and inhibits tumor growth. It could increase the concentration of local drug delivery in the targeted tumor areas, minimize harmful systemic side effects in normal tissues, and reduce the required drug doses and side effects during routine application of whole-body chemotherapy. Therefore, low-frequency ultrasound combined with chemotherapy may have broad application prospects in the future.

Authors' contributions: SZ conceived the study. SJ and ZJ carried out the animal experiments. QW did the clinical therapy. SZ wrote the manuscript. All authors approved the final submission.

DECLARATION OF CONFLICTING INTERESTS

The author(s) declared no potential conflicts of interest with respect to the research, authorship, and publication of this article.

FUNDING

The author(s) disclosed receipt of the following financial support for the research, authorship, and/or publication of this article: This study was funded in part by Six Talent Peaks Project in Jiangsu Province (Grant No. 2015-WSW-081); Nantong Municipal Science and Technology Project (Grant No. MS12016033); Nantong Health Committee Research Project (Grant No. MB2019018) and Nantong University clinical medicine project (2019LY033).

ORCID iD

Zhiyong Shen https://orcid.org/0000-0003-2570-7216

REFERENCES

1. Elmore S. Apoptosis: a review of programmed cell death. *Toxicol Pathol* 2007;**35**:495–516
2. Ei-Emshaty HM, Saad EA, Toson EA, Abdel MC, Gadelhak NA. Apoptosis and cell proliferation: correlation with BCL-2 and P53 oncoprotein expression in human hepatocellular carcinoma. *Hepatogastroenterology* 2014;**61**:1393–401
3. Michaeli J, Shaul ME, Mishalian I, Hovav AH, Levy L, Zolotriov L, Granot Z, Fridlender ZG. Tumor-associated neutrophils induce apoptosis of non-activated CD8 T-cells in a TNFalpha and NO-dependent mechanism, promoting a tumor-supportive environment. *Oncoimmunology* 2017;**6**:e1356965
4. Singh N, Sarkar J, Sashidhara KV, Ali S, Sinha S. Anti-tumour activity of a novel coumarin-chalcone hybrid is mediated through intrinsic apoptotic pathway by inducing PUMA and altering bax/bcl-2 ratio. *Apoptosis* 2014;**19**:1017–28
5. Chen ZY, Wang YX, Zhao YZ, Yang F, Liu JB, Lin Y, Liao JY, Liao YY, Zhou QL. Apoptosis induction by ultrasound and microbubble mediated drug delivery and gene therapy. *Curr Mol Med* 2014;**14**:723–36
6. Shi M, Liu B, Liu G, Wang P, Yang M, Li Y, Zhou J. Low intensity-pulsed ultrasound induced apoptosis of human hepatocellular carcinoma cells in vitro. *Ultrasonics* 2016;**64**:43–53
7. Tang W, Liu Q, Zhang J, Cao B, Zhao P, Qin X. In vitro activation of mitochondria-caspase signaling pathway in sonodynamic therapy-induced apoptosis in sarcoma 180 cells. *Ultrasonics* 2010;**50**:567–76
8. Ashush H, Rozenszajn LA, Blass M, Barda-Saad M, Azimov D, Radnay J, Zipori D, Rosenschein U. Apoptosis induction of human myeloid leukemic cells by ultrasound exposure. *Cancer Res* 2000;**60**:1014–20
9. Polat BE, Hart D, Langer R, Blankschtein D. Ultrasound-mediated transdermal drug delivery: mechanisms, scope, and emerging trends. *J Control Release* 2011;**152**:330–48
10. Bai WK, Zhang W, Hu B, Ying T. Liposome-mediated transfection of wild-type P53 DNA into human prostate cancer cells is improved by low-frequency ultrasound combined with microbubbles. *Oncol Lett* 2016;**11**:3829–34
11. Yang M, Xie S, Adhikari VP, Dong Y, Du Y, Li D. The synergistic fungicidal effect of low-frequency and low-intensity ultrasound with amphotericin B-loaded nanoparticles on *C. albicans* in vitro. *Int J Pharm* 2018;**542**:232–41
12. Tzanakis I, Lebon GS, Eskin DG, Pericleous KA. Characterizing the cavitation development and acoustic spectrum in various liquids. *Ultrason Sonochem* 2017;**34**:651–62
13. Zhao R, Liang X, Zhao B, Chen M, Liu R, Sun S, Yue X, Wang S. Ultrasound assisted gene and photodynamic synergistic therapy with multifunctional FOXA1-siRNA loaded porphyrin microbubbles for

enhancing therapeutic efficacy for breast cancer. *Biomaterials* 2018;**173**:58–70
14. Zhao L, Feng Y, Shi A, Zong Y, Wan M. Apoptosis induced by microbubble-assisted acoustic cavitation in K562 cells: the predominant role of the cyclosporin A-dependent mitochondrial permeability transition pore. *Ultrasound Med Biol* 2015;**41**:2755–64
15. Shen ZY, Shen E, Zhang JZ, Bai WK, Wang Y, Yang SL, Nan SL, Lin YD, Li Y, Hu B. Effects of low-frequency ultrasound and microbubbles on angiogenesis-associated proteins in subcutaneous tumors of nude mice. *Oncol Rep* 2013;**30**:842–50
16. Chen ZY, Liang K, Qiu RX. Targeted gene delivery in tumor xenografts by the combination of ultrasound-targeted microbubble destruction and polyethylenimine to inhibit survivin gene expression and induce apoptosis. *J Exp Clin Cancer Res* 2010;**29**:152
17. Zhang L, Li Y, Qiao L, Zhao Y, Wei Y, Li Y. Protective effects of hepatic stellate cells against cisplatin-induced apoptosis in human hepatoma G2 cells. *Int J Oncol* 2015;**47**:632–40
18. Wu KY, Wang HZ, Hong SJ. Mechanism of mitomycin-induced apoptosis in cultured corneal endothelial cells. *Mol Vis* 2008;**14**:1705–12
19. Shigeishi H, Biddle A, Gammon L, Rodini CO, Yamasaki M, Seino S, Sugiyama M, Takechi M, Mackenzie IC. Elevation in 5-FU-induced apoptosis in head and neck cancer stem cells by a combination of CDHP and GSK3beta inhibitors. *J Oral Pathol Med* 2015;**44**:201–7
20. Hu Z, Lv G, Li Y, Li E, Li H, Zhou Q, Yang B, Cao W. Enhancement of anti-tumor effects of 5-fluorouracil on hepatocellular carcinoma by low-intensity ultrasound. *J Exp Clin Cancer Res* 2016;**35**:71
21. Wood AK, Sehgal CM. A review of low-intensity ultrasound for cancer therapy. *Ultrasound Med Biol* 2015;**41**:905–28
22. Stride EP, Coussios CC. Cavitation and contrast: the use of bubbles in ultrasound imaging and therapy. *Proc Inst Mech Eng H* 2010;**224**:171–91
23. Staples BJ, Roeder BL, Husseini GA, Badamjav O, Schaalje GB, Pitt WG. Role of frequency and mechanical index in ultrasonic-enhanced chemotherapy in rats. *Cancer Chemother Pharmacol* 2009;**64**:593–600
24. Tomizawa M, Shinozaki F, Motoyoshi Y, Sugiyama T, Yamamoto S, Sueishi M. Sonoporation: gene transfer using ultrasound. *World J Methodol* 2013;**3**:39–44
25. Shen ZY, Shen E, Diao XH, Bai WK, Zeng MX, Luan YY, Nan SL, Lin YD, Wei C, Chen L, Sun D, Hu B. Inhibitory effects of subcutaneous tumors in nude mice mediated by low-frequency ultrasound and microbubbles. *Oncol Lett* 2014;**7**:1385–90
26. Liu H, Xu HW, Zhang YZ, Huang Y, Han GQ, Liang TJ, Wei LL, Qin CY, Qin CK. Ursodeoxycholic acid induces apoptosis in hepatocellular carcinoma xenografts in mice. *World J Gastroenterol* 2015;**21**:10367–74
27. Qiu DM, Wang GL, Chen L, Xu YY, He S, Cao XL, Qin J, Zhou JM, Zhang YX, EQ. The expression of beclin-1, an autophagic gene, in hepatocellular carcinoma associated with clinical pathological and prognostic significance. *BMC Cancer* 2014;**14**:327
28. Zhang K, Xu H, Chen H, Jia X, Zheng S, Cai X, Wang R, Mou J, Zheng Y, Shi J. CO2 bubbling-based 'nanobomb' system for targetedly suppressing panc-1 pancreatic tumor via low intensity ultrasound-activated inertial cavitation. *Theranostics* 2015;**5**:1291–302
29. Junhua A, Yun J, Zhenzhou W, Ling Y, Ding L. Treatment of malignant liver tumors by radiofrequency ablation combined with low-frequency ultrasound radiation with microbubbles. *PLoS One* 2013;**8**:e53351
30. Feng Q, Zhang W, Yang X, Li Y, Hao Y, Zhang H, Hou L, Zhang Z. pH/ultrasound dual-responsive gas generator for ultrasound imaging-guided therapeutic inertial cavitation and sonodynamic therapy. *Adv Healthc Mater* 2018;**7**. doi: 10.1002/adhm.201700957
31. Shen ZY, Xia GL, Hu B, Xie YG, Wu MF. Preoperative ultrasound features as prognostic factors for patients with hepatocellular carcinoma. *Radiol Med* 2015;**120**:504–10
32. Shen ZY, Jiang YM, Zhou YF, Si HF, Wang L. High-speed photographic observation of the sonication of a rabbit carotid artery filled with microbubbles by 20-kHz low frequency ultrasound. *Ultrason Sonochem* 2018;**40**:980–7
33. Yan M, Ni J, Song D, Ding M, Huang J. Activation of unfolded protein response protects osteosarcoma cells from cisplatin-induced apoptosis through NF-kappaB pathway. *Int J Clin Exp Pathol* 2015;**8**:10204–15
34. McKenna E, Traganos F, Zhao H, Darzynkiewicz Z. Persistent DNA damage caused by low levels of mitomycin C induces irreversible cell senescence. *Cell Cycle* 2012;**11**:3132–40
35. Dun J, Chen X, Gao H, Zhang Y, Zhang H, Zhang Y. Resveratrol synergistically augments anti-tumor effect of 5-FU in vitro and in vivo by increasing S-phase arrest and tumor apoptosis. *Exp Biol Med* 2015;**240**:1672–81
36. Guclu H, Doganlar ZB, Gurlu VP, Ozal A, Dogan A, Turhan MA, Doganlar O. Effects of cisplatin-5-fluorouracil combination therapy on oxidative stress, DNA damage, mitochondrial apoptosis, and death receptor signalling in retinal pigment epithelium cells. *Cutan Ocul Toxicol* 2018;**37**:291–304
37. Snipstad S, Berg S, Morch Y, Bjorkoy A, Sulheim E, Hansen R, Grimstad I, van Wamel A, Maaland AF, Torp SH, Davies CL. Ultrasound improves the delivery and therapeutic effect of Nanoparticle-Stabilized microbubbles in breast cancer xenografts. *Ultrasound Med Biol* 2017;**43**:2651–69
38. Shen ZY, Xia GL, Wu MF, Ji LY, Li YJ. The effects of percutaneous ethanol injection followed by 20-kHz ultrasound and microbubbles on rabbit hepatic tumors. *J Cancer Res Clin Oncol* 2016;**142**:373–8
39. Liu L, Huang Z, Chen J, Wang J, Wang S. Protein phosphatase 2A mediates JS-K-induced apoptosis by affecting bcl-2 family proteins in human hepatocellular carcinoma HepG2 cells. *J Cell Biochem* 2018;**119**:6633–43
40. Zhao G, Zhu Y, Eno CO, Liu Y, Deleeuw L, Burlison JA, Chaires JB, Trent JO, Li C. Activation of the proapoptotic bcl-2 protein bax by a small molecule induces tumor cell apoptosis. *Mol Cell Biol* 2014;**34**:1198–207
41. Ren ST, Shen S, He XY, Liao YR, Sun PF, Wang B, Zhao WB, Han SP, Wang YL, Tian T. The effect of docetaxel-loaded micro-bubbles combined with low-frequency ultrasound in H22 hepatocellular carcinoma-bearing mice. *Ultrasound Med Biol* 2016;**42**:549–60
42. Liu ZY, Weng CX, Chen W, Zhao HY, Li T. Low-Frequency ultrasound enhances paclitaxel efficacy in EMT6 subcutaneous tumors in balb/c mice. *Oncol Res Treat* 2016;**39**:204–8
43. Shen ZY, Xia GL, Wu MF, Shi MX, Qiang FL, Shen E, Hu B. The effects of low-frequency ultrasound and microbubbles on rabbit hepatic tumors. *Exp Biol Med* 2014;**239**:747–57
44. Sahara S, Kawai N, Sato M, Tanaka T, Ikoma A, Nakata K, Sanda H, Minamiguchi H, Nakai M, Shirai S, Sonomura T. Prospective evaluation of transcatheter arterial chemoembolization (TACE) with multiple anti-cancer drugs (epirubicin, cisplatin, mitomycin c, 5-fluorouracil) compared with TACE with epirubicin for treatment of hepatocellular carcinoma. *Cardiovasc Intervent Radiol* 2012;**35**:1363–71
45. Lee TK, Na KS, Kim J, Jeong HJ. Establishment of animal models with orthotopic hepatocellular carcinoma. *Nucl Med Mol Imaging* 2014;**48**:173–9
46. Reiberger T, Chen Y, Ramjiawan RR, Hato T, Fan C, Samuel R, Roberge S, Huang P, Lauwers GY, Zhu AX, Bardeesy N, Jain RK, Duda DG. An orthotopic mouse model of hepatocellular carcinoma with underlying liver cirrhosis. *Nat Protoc* 2015;**10**:1264–74
47. Shen ZY, Wu MF, Zhang YX, Shen K, Xia GL. Treatment of hepatic carcinoma by low-frequency ultrasound and microbubbles: a case report. *Oncol Lett* 2015;**9**:1249–53

(Received March 24, 2020, Accepted June 1, 2020)